Changes in motor unit behavior following isometric fatigue of the first dorsal interosseous muscle

by

Lara McManus [1], Xiaogang Hu [2], William Z. Rymer [2, 3], Madeleine M. Lowery [1], Nina L. Suresh [2]

1) University College Dublin, Belfield, Dublin 4, Ireland
2) Rehabilitation Institute of Chicago, Chicago, IL 60611, USA
3) Northwestern University, Evanston, IL 60208, USA

Abbreviated Title: Changes in motor unit action potentials following fatigue

Corresponding Author: Ms. Lara McManus

University College Dublin, Belfield, Dublin 4, Ireland

lara.mc-manus@ucdconnect.ie

Phone: (353) 1 716 1938

Number of text pages: 20, figures: 8

Number of words: abstract: 248, introduction: 1155, discussion: 2046

Total number of words: 7268

Acknowledgements: The authors declare no competing financial interests.

Grants: Funding provided by the Irish Research Council.

Author contributions: L.M., M.M.L. and N.L.S. conception and design of research; L.M., X.H. and N.L.S. performed experiments; L.M., X.H. and N.L.S. analyzed data; L.M., M.M.L., W.Z.R. and N.L.S. interpreted results of experiments; L.M. prepared figures; L.M., M.M.L. and N.L.S. drafted manuscript; L.M., M.M.L., N.L.S. and W.Z.R. edited and revised manuscript; L.M., M.M.L., W.Z.R., X.H. and N.L.S. approved final version of manuscript.

ABSTRACT The neuro-muscular strategies employed to compensate for fatigue-induced muscle force deficits are not clearly understood. This study utilizes surface electromyography (sEMG) together with recordings of a population of individual motor unit action potentials (MUAPs) to investigate potential compensatory alterations in motor unit (MU) behavior immediately following a sustained fatiguing contraction, and after a recovery period.

EMG activity was recorded during abduction of the First Dorsal Interosseous in 12 subjects at 20% maximum voluntary contraction (MVC), before and directly after a 30% MVC fatiguing contraction to task failure, with additional 20% MVC contractions following 10 minutes rest. The amplitude, duration and mean firing rate (MFR) of MUAPs extracted with a sEMG decomposition system were analyzed, together with sEMG root-mean-square (RMS) amplitude and median frequency (MPF).

MUAP duration and amplitude increased immediately post-fatigue, and were correlated with changes to sEMG MPF and RMS respectively. After 10 minutes, MUAP duration and sEMG MPF recovered to pre-fatigue values but MUAP amplitude and sEMG RMS remained elevated. MU MFR and recruitment thresholds decreased post-fatigue and recovered following rest.

The increase in MUAP and sEMG amplitude likely reflects recruitment of larger MUs, while recruitment compression an additional compensatory strategy directly post-fatigue. Recovery of MU MFR in parallel with MUAP duration suggests a possible role for metabolically sensitive afferents in MFR depression post-fatigue.

This study provides insight into fatigue-induced neuromuscular changes by examining the properties of a large population of concurrently recorded single MUs, and outlines possible compensatory strategies involving alterations in MU recruitment and MFR.

Key words: Motor unit action potential, surface electromyography decomposition, isometric fatigue

INTRODUCTION

Adaptations in motor unit (MU) recruitment and firing rate modulation during contraction-induced fatigue have been proposed as compensatory mechanisms counteracting the decline in muscle force generating capacity. The progressive recruitment of new MUs during fatiguing contractions performed at a submaximal level has been demonstrated in a number of studies, employing both sustained (Garland et al. 1994; Jensen et al. 2000; Maton and Gamet 1989) and intermittent (Adam and De Luca 2003; Bigland-Ritchie et al. 1986b; Carpentier et al. 2001; Christova and Kossev 1998; Dorfman et al. 1990; Enoka et al. 1989) fatiguing protocols. This recruitment appears to compensate for fatigue-induced loss, and to aid in preserving force generation.

The role of alterations in MU firing rate and recruitment threshold in response to fatigue are less clearly defined. It has been suggested that these changes are not uniform across the motor unit pool (Carpentier et al. 2001; Garland et al. 1994) and that adjustments to individual MUs may depend on activation history (Farina et al. 2009). During sustained and intermittent voluntary contractions, motor units active from the beginning of the contraction typically exhibit a decline in discharge rate (Carpentier et al. 2001; Enoka et al. 1989; Garland et al. 1994), however newly recruited MUs have been shown to exhibit a range of behaviors. Later recruited MUs have been reported to fire at a constant rate or even to increase steadily (Garland et al. 1994), to exhibit no significant change in discharge rate (Adam and De Luca 2005), or to show varying rates with time (Carpentier et al. 2001). Although a decrease in the recruitment threshold of higher threshold MUs following fatigue is generally reported (Adam and De Luca 2003; Calder et al. 2008; Carpentier et al. 2001; Jensen et al. 2000), some studies have observed increased recruitment thresholds for early recruited MUs (Carpentier et al. 2001; Farina et al. 2009). Others have reported a homogenous and monotonic decrease in the recruitment threshold of their sample motor unit population as fatigue progressed (Adam and De Luca 2003; Christova and Kossev 1998).

A key factor that may account for the variations observed could be the type of motor unit recordings that are utilized. The use of surface EMG is often preferred over intramuscular recordings as a more

stable recording during dynamic or fatiguing contractions, with surface EMG providing a summary representation of motor unit behavior. Yet, in order to gain a comprehensive view of compensatory recruitment and firing rate strategies, it is imperative to analyze changes occurring at the motor unit level. These in turn can provide context from which to interpret the adaptations in the sEMG signal.

Recent advances in surface EMG decomposition methods have provided a promising new method for analyzing the activity of individual motor units without the limitations associated with intramuscular EMG. A number of different surface EMG configurations have been employed to-date (Gazzoni et al. 2004; Hogrel 2003; Holobar et al. 2009; Kleine et al. 2008; Nawab et al. 2010). Kallenberg and Hermens (2008) observed an increase in the number of MUAPs detected per second over the course of a sustained fatiguing contraction in the biceps brachii. Although the method collectively considered both MU recruitment and firing rate, the corresponding increase in the mean root mean-squared (RMS) amplitude of identified MUAPs suggests recruitment was the primary factor in maintaining force output. Calder et al. (2008) used a decomposition-based algorithm to identify firing times of individual MUs, and extracted corresponding MUAPs by spike trigger averaging the sEMG signal from the biceps brachii. They similarly reported that increases in mean MUAP amplitude and area were mirrored by increases in the sEMG signal amplitude as the contractions progressed. This was accompanied by a significant decrease in mean MU firing rates, despite a constant torque output. A reduction in mean firing rates was also reported for MUAPs detected in the Vastus Lateralis, but not in the Vastus Medialis, in response to an intermittent fatiguing protocol (Stock et al. 2012).

It has not yet been evaluated whether a systematic approach to MU firing rate modulation and MU recruitment strategies is employed to compensate for force deficits in a fatigued muscle, due partly to the varied fatiguing protocols employed. In particular, it remains unclear whether firing rate adaptations due to fatigue are uniform across the motoneuron pool and whether there are simultaneous changes in MU recruitment strategies, such as compressed recruitment and/or recruitment of larger motor units. For technical reasons, compensatory mechanisms in a fatigued muscle have not yet been systematically assessed over a large population of concurrently recorded units.

97 To address these questions, the objective of our study was to compare MU behavior directly after
98 isometric fatigue, and following partial recovery, to pre-fatigue conditions in the First Dorsal
99 Interosseous (FDI) muscle. The aim of this approach is to comprehensively assess the relative
100 contribution of MU firing rate and recruitment strategies in accommodating for muscle force
101 impairment in a fatigued hand muscle. In addition, the ability to record a large sample MU population
102 using a sEMG decomposition system (dEMG) allows us to determine the degree of uniformity of
103 these adaptations across the MU pool.

104 This study characterizes the response of a population of motor units following isometric fatigue using
105 a dEMG system that utilizes a novel surface sensor array recording electrode, coupled with advanced
106 pattern recognition software to identify single MUAPs. The dEMG approach has been validated with
107 a range of different techniques (De Luca and Nawab 2011; Hu et al. 2013a; b), using a two-source
108 recording method (Hu et al. 2014), as well as several advanced simulation studies. It has been used to
109 investigate the control of multiple motor units in voluntary contractions under in intact subjects (De
110 Luca and Hostage 2010; Defreitas et al. 2014), during fatigue (Beck et al. 2012; Stock et al. 2012) and
111 in stroke survivors (Hu et al. 2012). The dEMG system allows motor unit behavior in a fatigued
112 muscle to be characterized using both the standard surface EMG signal and information from
113 individual MUAPs. The relationship between the two recordings can also be examined to determine
114 which MU properties predominate in mediating the changes in the sEMG signal.

115 Our results show an increase in sEMG and MUAP amplitude post-fatigue and following a recovery
116 period, indicating the recruitment of larger motor units to compensate for the decline in the force
117 generating capacity of the fatigued muscle. MUAP duration increased directly post-fatigue, but
118 recovered after the rest period, suggesting the restoration of the ionic and metabolic changes to the
119 muscle that slow muscle fiber conduction velocity (MFCV). This was accompanied by a parallel
120 decrease and subsequent increase in MU firing rates, consistent across the MU pool. The reduction in
121 firing rates coupled with continued recruitment may suggest a selective inhibition of early recruited
122 motoneurons, mediated through increased activity of mechanically and metabolically sensitive
123 afferents. The results indicate that a combination of supplementary MU activation and lower MU

recruitment threshold is favored over rate-coding to maintain the force after fatigue while motor units are available.

METHODS

Participants

Twelve right-dominant neurologically intact individuals (6 male, 6 female) volunteered to participate in this study. The force and EMG activity of the first dorsal interosseous muscle were examined during isometric abduction of the right index finger about the 2nd metacarpo-phalangeal (MCP) joint. All participants gave informed consent via protocols approved by the Institutional Review Board under the Office for the Protection of Human Subjects at Northwestern University.

Experimental Setup

Participants were seated upright in a Biodex experimental chair (Biodex Medical systems, Shirley, NY) with their upper arm comfortably resting on a plastic support. To standardize hand position and to minimize contributions of unrecorded muscles, the forearm was cast and placed in a ring mount interface attached to an elbow rest at the wrist. The elbow rest was securely mounted with magnetic stands to a heavy steel table. The forearm was placed in full pronation and the wrist was held neutral with respect to flexion/extension. The little, ring and middle fingers were separated from the index finger and strapped to the support surface. The thumb was secured at an approximately 60-degree angle to the index finger. The index finger was placed in line with the 2nd metacarpal and the long axis of the forearm creating a 0 degree or neutral (abduction/adduction) MCP joint angle. The proximal phalanx of the index finger was fixed to a ring-mount interface attached to a six degrees-of-freedom load cell (ATI, Inc., 3226). Recorded forces from the x (abduction/adduction) and y (extension/flexion) directions were low pass filtered (cut-off =200 Hz) and digitized at a sampling frequency of 1 kHz. The subjects were instructed to produce required abduction forces while minimizing the off-axis forces. There is evidence that both motor unit recruitment threshold (Enoka et al. 1989) and patterns of recruitment (Suresh et al. 2002) are directionally dependent (i.e. finger flexion vs. abduction) in the FDI. In order to prevent variations in rank order of MU recruitment with

different directions of contraction (Thomas et al. 2006) off-axis forces in the flexion direction were tightly controlled. The subject received visual feedback of the force in the x and y direction (flexion/extension), to minimize off axis forces and maximize the force exerted in the desired x direction.

The subject's skin was prepared using adhesive tape and alcohol pads. Surface EMG was recorded from the FDI using a surface sensor array (Delsys, Inc.) that consisted of 5 cylindrical probes (0.5 mm diameter) located at the corners and at the center of a 5 × 5 mm square (Nawab et al. 2010). Pairwise differentiation of the 5 electrodes yielded 4 channels of sEMG signals (Figure 1 (a)). The sEMG sensor and a reference electrode were connected to 4 channels of a Bagnoli sEMG system (Delsys, Inc.). The signals were amplified and filtered between 20 Hz and 2 kHz. The signals were sampled at 20 kHz and stored on a computer for further processing.

Protocol

Subjects were asked to perform a series of three maximal voluntary contractions (MVCs) for 3 s, with 1 min rest between trials, and the largest value was designated as 100 % MVC. The subjects were then asked to perform a series of six isometric voluntary contractions in which they followed a trapezoidal force trajectory as depicted in Figure 1 (b), in order to provide a pre-fatigue baseline. Feedback on the force direction and magnitude was presented to the subject in two-dimensional display on a computer screen as a visual aid. The dimensions of the target on screen were kept constant across subjects, therefore visual gain was maintained over the experiment for a single subject but varied between subjects according to subject MVC. Previous studies have indicated that alterations to visual gain can influence force fluctuations (Sosnoff and Newell, 2009) and motoneuronal excitability (Laine et al., 2014). However, in this study inter-subject differences in visual feedback were relatively small and were unlikely to have had significant effects on force variability (Baweja et al., 2009). The trapezoid trajectory contained 5 segments: a 3 s quiescent period for baseline noise calculation, an up-ramp increasing at a rate of 10% MVC/s, a constant force of 20% MVC for 10 s, a down-ramp decreasing at 10% MVC/s, and a final 3 s quiescent period. To

ensure that the subjects could trace the trapezoid trajectory closely, they were given practice trials before the main experiment. During this section of the experiment, the subject was given a 1-minute rest period between repetitions to minimize fatigue. After the six pre-fatigue trials, a sustained isometric contraction was performed at 30% MVC to task failure in order to induce fatigue. The subjects were given visual bar feedback of their force output and the time of task failure was defined as the time when the subject's force dropped 10% below the required output for a period of 5 or more seconds. A single MVC was performed directly following task failure, and six post-fatigue trapezoidal force trajectories at 20% MVC were subsequently performed, with no rest period given between trials to minimize recovery. The subjects were then allowed a 10-minute recovery period before a series of four more trapezoidal trajectories (20% MVC) was performed. A final maximum voluntary contraction was recorded in 10 of the subjects following the recovery trials.

Figure 1

Data Analysis

To be selected for further analysis, surface EMG signals were required to have a peak to peak (P-P) baseline noise < 20 μV and signal to noise ratio > 5 with no sudden change (i.e., larger than 20% MVC/s) in the up-ramp force. The analysis was confined to the surface EMG signals recorded before and directly after the fatiguing contraction, and following the recovery period, in order to adhere to specific experimental conditions for which the dEMG system has been previously validated, i.e. short duration isometric contractions. Next, discriminable MUs were extracted using the dEMG decomposition system (version 1.0.0.28). For each identified MU, the output of the algorithm consisted of MU firing times and 4 MUAP waveforms (for the 4 recorded channels). Detailed information for the decomposition algorithms is described in Nawab et al. (2010) and De Luca and Hostage (2010).

Spike triggered averaging (STA) of the sEMG was performed to characterize the MU waveform recorded from the surface electrodes. A STA was performed on each of the 4 channels of the sEMG signals, using the identified firing times for each MU as triggers, resulting in 4 representative STA

MUAP estimates for each MU. The time interval used to derive the template estimate was 10 ms prior to and after the firing time. The peak-to-peak amplitude was calculated as the voltage difference between the maximum peak and the adjacent minimum peak within the time window. The time between the nearest zero crossings to the maximum and minimum peaks was calculated to provide the MUAP duration.

Two separate reliability tests were performed to determine which decomposed MUAP estimates would be retained for further analysis, using the procedure outlined in Hu et al. (2013b). To quantify the variation of the STA MUAP over time, the coefficient of variation (CV) was calculated for the peak-to-peak (P-P) amplitude of the MUAP templates. This coefficient was implemented as a measure of the stability of the waveform average over the duration of the contraction and the accuracy of the firing time estimation. The maximum linear correlation coefficient between the STA estimate (calculated over the entire trial duration) and the decomposition-estimated templates was computed as a second measure of the reliability of the STA estimates of the MUAP. The MUs with a correlation coefficient (between the STA MUAP estimate and the decomposition MU template) >0.7 and CV of P-P <0.3 across all four channels were selected for later analysis. The average correlation coefficient between the STA MUAP and MU template, as well as the average CV of P-P amplitude derived from each of the four channels, was used to qualify each MU for use in further analysis. For each identified MU, the combined results from all four channels was used only for the MU selection process, subsequent analysis of the selected MUs was simplified by using the channel of maximum median amplitude for each subject.

The recruitment threshold was defined as the threshold force at recruitment, calculated as the averaged force over the interval -50 to +100 ms relative to the first firing event. The mean firing rate was calculated with a non-overlapping window of 0.5 s length from a 4-s averaging window in the middle of the steady state hold phase of the contraction. The relationship between the MUAP amplitude/duration and the recruitment threshold force of the MU was examined by fitting a linear regression line to the data and calculating the slope and r squared values of the fit.

To assess the relationship between spectral properties of the global signal and characteristics of the decomposed MUAPs, the mean RMS and the median frequency of the power spectrum (MPF) value of the sEMG signal during the trapezoidal force trajectories were calculated for each subject, for each of the three conditions (pre-, post-fatigue, and recovery). The average values were obtained using a 1 second moving average window and step size of 0.5 s over 2 seconds of the steady state hold phase (7-9 s) using the first trial at 20% MVC.

The RMS value of the EMG signal was calculated across a 1 second time window (5-6 s) during the 30% MVC fatiguing contraction for each subject. In order to control for between-subject variations in sEMG amplitude, this RMS value was used to normalize the RMS amplitude of the global signal detected for each condition. The mean and standard deviation of the decomposed MUAP amplitudes were calculated for the MUs detected in the pre-fatigue condition for each subject and used to standardize the pre-fatigue MUAP amplitude distribution to have a zero mean and unit variance. The pre-fatigue mean and standard deviation were then used to standardize the post-fatigue and recovery MUAP distributions within the same subject. Standardized distributions were used to examine the changes in MUAP amplitude with condition across subjects and reduce subject specific variability in the mean and variance of the distribution.

Statistics

For each subject, the median value of the MPF and RMS of the global sEMG signal and the amplitude and duration of the surface decomposed MUAPs were calculated for the pre-fatigue, post-fatigue and recovery states. The probability distributions of the decomposed MUAP amplitudes and durations were analyzed per condition for each subject. A one-way within-subjects (or repeated measure) analysis of variance (ANOVA) was conducted to compare the effect of condition on each parameter across subjects, with a statistic test for pre-fatigue, post-fatigue and recovery states. Mauchly's Test of Sphericity was implemented to check the assumption of sphericity, and if violated, a Greenhouse-Geisser correction was applied to the data. Post hoc tests to examine pairwise differences between conditions were conducted using the Fisher's Least Significant Difference (LSD) test. A regression

analysis using a generalized linear model was performed to examine the change of MPF and RMS of sEMG during the fatigue protocol.

RESULTS

The properties of the sEMG signal and the characteristics of multiple discriminated MU spike trains, including mean firing rates and the estimated threshold force, were examined before and after a fatiguing contraction. The alterations in median MUAP amplitude and duration were related to the changes observed in the RMS amplitude and mean frequency of the surface signal. Changes in MUAP amplitude and duration and MU firing rate were examined as a function of MU recruitment threshold to assess the uniformity of the adaptations across the MU pool.

Force Properties

Changes in subject MVC across the conditions (for n=10 subjects) were analyzed with an ANOVA before and after the sustained isometric 30% MVC fatiguing contraction to task failure (196.8 ± 55 seconds). The results indicate a significant difference in subject MVC between pre- and post-fatigue conditions ($F(2, 18) = 33.895$, $p < .0001$). Post hoc tests revealed a significant reduction ($p < .001$) in MVC following fatigue (54.15 ± 11.53 N to 30.43 ± 13.36 N, respectively). The median subject MVC failed to recover after the period of rest and remained significantly depressed (42.75 ± 16.75 N, $p < .001$) compared to initial pre-fatigue values, though higher than that recorded directly post-fatigue ($p < 0.005$).

Figure 2

Surface EMG signal

The results of an ANOVA, with Greenhouse-Geisser correction show that there was a significant effect of condition (pre-fatigue, post-fatigue and recovery) on the EMG MPF, ($F(1.18, 12.99) = 20.123$, $p < .0001$) (Figure 2 (a)). Post hoc tests revealed that the sustained, fatiguing contraction resulted in a significant decrease in global signal MPF from pre-fatigue to post-fatigue conditions (166.9 ± 52.09 Hz to 100.38 ± 31.42 Hz, respectively, $p < .001$, standardized values 0 ± 1 to -1.27 ± .6). However, after the recovery period the MPF increased significantly (170.87 ± 79.04 Hz, $p = .002$,

standardized value 0.08 ± 1.5), and was found not to be statistically different from MPF values before fatigue ($p = .709$).

ANOVA on the mean scores for normalized RMS amplitudes also confirmed a significant effect of condition ($F(2, 22) = 7.08$, $p = .004$) (Figure 2 (b)). Median normalized RMS amplitude increased significantly ($p = .023$) from pre-fatigue to post-fatigue conditions (1.01 ± 0.075 to 1.36 ± 0.47 and 0.19 ± 0.18 to 0.26 ± 0.14, normalized and non-normalized values, respectively). After the period of 10 minutes recovery mean RMS amplitude (1.49 ± 0.56, normalized, 0.29 ± 0.13, non-normalized) remained elevated with respect to the initial RMS mean ($p = .012$), however, the values were not significantly different to post-fatigue values ($p = .198$).

Figure 3

Figure 4

Decomposed MUAPs

Within each condition pre-fatigue, post-fatigue and after the recovery period, 78.6% (1164 of 1480 MUs), 76% (1052 of 1384 MUs) and 78% (784 of 1001 MUs) were accepted respectively. Unless otherwise stated the values reported are based on the analysis of accepted units. Over all conditions, 77% of decomposed motor units met the criteria to be accepted for further analysis. The probability density distribution in Figure 3 displays the probability of occurrence of an accepted MU of a particular amplitude plotted against increasing amplitude values in a single representative subject, and across all subjects for pre-fatigue, post-fatigue and after 10 minutes recovery. Boxplots display the mean (line), median ('+'), standard deviation and outliers of the distribution for the indicated MU population. Figure 4 shows the corresponding probability distribution of the MU durations in a single representative subject and across all subjects.

Figure 5

Repeated measures ANOVAs were then employed to examine the intrinsic signal properties of the decomposed MUAPs. The change in MVC (Figure 5 (a)) was accompanied by a significant change in

the duration of the decomposed MUAPs with condition ($F(2, 22) = 79.97$, $p < .0001$) (Figure 5 (b)). Median MU duration increased significantly ($p < .0001$) from pre-fatigue to post-fatigue conditions (7.05 ± 1.29 ms vs. 10.21 ± 2.03 ms, respectively). However, after the recovery period median MU durations then decreased significantly (7.26 ± 1.74 ms, $p < .0001$), and were found not to be statistically different from durations observed before fatigue ($p = 0.329$).

The results of an RM ANOVA, with Greenhouse-Geisser correction, on the median standardized amplitudes of decomposed MUs reveal that the median MUAP amplitude was significantly affected by fatigue ($F(1.3, 14.3) = 7.57$, $p = .01$) (Figure 5 (c)). An increase in median standardized MU amplitude was observed from pre-fatigue to post-fatigue conditions (-0.2 ± 0.058 vs. $0.46 \pm .97$, respectively), which was statistically significant ($p < .05$). However, after the period of 10 minutes recovery MUAP amplitudes (0.7 ± 0.99) remained significantly higher than pre-fatigue values ($p < .01$). No statistical difference was observed between the medians of the two sets of MUAP amplitudes recorded after the fatiguing contraction, whether recorded directly after or following the recovery period ($p = .068$).

In order to investigate whether there was any systematic bias in the method employed to retain MUs for further analysis, the ANOVAs were repeated using all of the original decomposed MUs. There was no difference in the direction of any of changes in MU amplitude or duration for each condition.

Figure 6

MU firing rate changes

Repeated measures ANOVAs were then employed to examine the mean firing rates over each condition. The results show that there was a significant effect of condition on the firing rates of the decomposed MUAPs ($F(2, 22) = 10.04$, $p < .001$), Figure 6 (b). Median MU mean firing rate decreased significantly ($p < .015$) from pre-fatigue to post-fatigue conditions (10.9 ± 1.26 Hz vs. 10.15 ± 1.47 Hz, respectively). However, after the recovery period median MU firing rates then increased significantly (11.23 ± 1.27 Hz, $p<.001$), and were found not to be statistically different from discharge rates observed before fatigue ($p = .218$).

The average firing rate of MUs was calculated within a bin width equal to 1% MVC for each subject over all conditions and the mean result for all subjects is displayed in Figure 6 (b). A significant negative correlation was observed between threshold of recruitment and average firing rates per bin for pre-fatigue, post-fatigue and recovery conditions ($r(101) = -.7$, $p < .001$, $r(85) = -.6$, $p < .001$ and $r(103) = -.73$, $p < .001$ respectively).

Figure 7

MU Recruitment Threshold

Figure 7 presents the probability distribution of the recruitment threshold for the MUAP pool. The results of a repeated measures ANOVA show a significant effect of condition on the median threshold of recruitment for decomposed MUAPs ($F(2, 22) = 3.497$, $p < .05$) (Figure 7). Median MU threshold of recruitment was significantly lower directly post fatigue (5.75 ± 2.06 % MVC) than both pre-fatigue and recovery conditions (7.83 ± 2.96 % MVC, $p < .05$, and 7.89 ± 3.09 % MVC, $p < .05$, respectively).

The normalized MUAP amplitude for each subject was binned with respect to its threshold of recruitment with a bin width of the normalized force equal to 1% MVC. The average MUAP amplitude in the post-fatigue and recovery conditions was greater than the corresponding pre-fatigue average at each threshold bin; however there was no consistent trend to suggest that lower or higher threshold MUs were affected disproportionately. Similarly, the increase in the average duration of MUAPs detected at each 1% MVC force interval after fatigue did not appear to be influenced by the initial MU recruitment threshold.

Effect of recruitment threshold on measured parameters

The uniformity of MUAP property changes across the MU pool were investigated by examining the relationship between the decomposed MUAP amplitude/duration and the recruitment threshold force of the MU. No correlation was observed between MUAP duration and recruitment threshold force, the linear regression slope did not differ significantly from zero for 96% of the trials. We found no

systematic change with condition for either the slope or the r-squared value of the linear regression fit to the MUAP amplitude versus threshold plot when analyzed with a RM ANOVA ($F(2, 22) = 2.62$, $p = .095$ and $F(2, 22) = .076$, $p = .927$ respectively). This may indicate compensatory strategies post-fatigue are subject specific, with a combination of recruitment compression (increased slopes) and supplementary MU recruitment (no change in slope values) employed. A significant increase in amplitude with threshold was observed in only 47% of trials, which may occur as a result of the low force of the contraction. Although no consistent change in the slope of the MUAP amplitude versus threshold plot was observed, higher mean slopes were reported directly post-fatigue (0.057 ± 0.07) and after recovery (0.039 ± 0.035), than the slopes observed pre-fatigue (0.029 ± 0.036). In contrast, similar mean r-squared values were reported for all three conditions (0.32 ± 0.26, 0.33 ± 0.2 and 0.32 ± 0.2; pre-fatigue, post-fatigue and after recovery respectively).

Co-variation of global surface EMG measures and MU parameters

An approximately linear relationship was observed between the median amplitude of decomposed MUAPs and the RMS amplitude of the global sEMG signal. The scatterplot in Figure 8 (a) presents the relationship between MUAP amplitude and sEMG amplitude for all of the three conditions, along with the Pearson product-moment correlation coefficient. A strong, statistically significant positive correlation was observed between MUAP amplitude and the amplitude of the sEMG signal, $r(36) = .86$, $p < .0001$. A Spearman's rank-order non-parametric correlation was performed to determine the non-linear but monotonic relationship between the median duration of decomposed MUAPs and the MPF of the global sEMG signal across each of the three conditions. The scatterplot in Figure 8 summarizes the results, a strong, statistically significant negative correlation was observed between MUAP duration and the median frequency of the global signal, $r(36) = -.95$, $p < .0001$.

The square of the Pearson product-moment correlation coefficient was computed to assess the approximately linear relationship between the median amplitude and firing rate of decomposed MUAPs and the percentage change between conditions for the median duration and firing rate of decomposed MUAPs. A strong, statistically significant negative correlation was observed between

MUAP amplitude and firing rate, $r(36) = -.4$, $p < .05$ and percentage change between conditions for MUAP duration and discharge rate, $r(36) = -.726$, $p < .0001$.

Figure 8

DISCUSSION

In this study, surface EMG and motor unit action potential properties, including motor unit recruitment and firing rates, were examined collectively to provide insight into changes due to isometric muscle fatigue and in the following recovery period. While many of these techniques are well established, the capacity to decompose the surface EMG signal into constituent motor unit action potentials offers a unique overview of the distribution of MUAP waveform characteristics across a large population of MUs, an approach that has been difficult to implement using traditional surface or intramuscular EMG methods to-date. The sEMG decomposition technique also allows a comprehensive, simultaneous analysis of firing rate and recruitment properties across the motor neuron pool, in a manner not previously attainable.

Changes to the Global EMG signal

For each subject, a sustained, fatiguing contraction induced a reduction in the force generating capacity of the FDI muscle immediately following the contraction. The reduction in maximal force persisted beyond the 10 minute recovery period (Figure 5 (a)). This incomplete recovery of force following a rest period has also been reported previously in the biceps brachii and the FDI muscles, using a similar sustained, submaximal fatiguing protocol (Esposito et al. 1998; Fuglevand et al. 1993b; Post et al. 2008). The presence of muscle fatigue is supported by a significant progressive decrease in the median frequency of the EMG signal during the sustained fatiguing contraction, and immediately post-fatigue (Figure 2 (a)). This is consistent with the well-established decline in muscle fiber conduction velocity as fatigue progresses. The sEMG spectral properties recorded immediately after the fatiguing contraction suggest a change in the metabolic and ionic state of the muscle, resulting in a depression of muscle fiber conduction velocity, and subsequently the MPF (Figure 2 (a)). After the rest period of 10 minutes, the MPF had recovered to pre-fatigue values. The frequency

411 compression of the power spectrum is primarily governed by shape alterations in the MUAP
412 waveforms that comprise the signal, with minimal influence from motor unit firing rates (Hermens et
413 al. 1992). The recovery of the MPF thus suggests that the MFCV and hence duration of the MUAP
414 have also been restored to pre-fatigue values.

415 The decline in MPF post-fatigue was accompanied by a simultaneous rise in surface EMG amplitude
416 (Figure 2 (b)). Although the complexity of the surface signal limits the utility of EMG amplitude as
417 an index of muscle activation, an increase during and immediately following sustained submaximal
418 contractions is usually considered to indicate an enhancement of the central drive (Bigland-Ritchie et
419 al. 1986b; Fuglevand et al. 1993a), though it can be influenced by surges in Na^+-K^+ pump activity,
420 MU synchronization and rate-coding, and prolonged duration of the underlying MUAP shape due to
421 decreased conduction velocity (Farina et al. 2004; Hicks and McComas 1989; Lowery and O'Malley
422 2003). This increase in the intensity of the central drive increases the number of motor units recruited
423 and/or modulates the firing rates of previously active MUs (Fuglevand et al. 1993b).

424 In the present study, a reduction in mean firing rates was observed post-fatigue which suggests that
425 MU rate coding was not a contributing factor to the rise in surface EMG amplitude (Gabriel and
426 Kamen 2009). However, the contribution of MU synchronization, which has been proposed to
427 increase following fatigue (Holtermann et al. 2009), in augmenting surface EMG amplitude cannot be
428 excluded. After a period of rest, surface EMG amplitude remained elevated, disparate from the
429 observed recovery of the signal frequency content. The decoupling of spectral and amplitude
430 properties provides evidence that changes in the muscle fiber action potential waveforms and
431 reduction in conduction velocity are not the primary factor responsible for the enlargement of the
432 EMG signal amplitude.

433 *Changes in MUAP Amplitude and Duration*

434 Properties of decomposed MUAP waveforms mirrored the changes observed in the global EMG
435 signal (Figure 8), and a strong correlation was observed between MUAP amplitude and RMS sEMG
436 (Figure 8 (a)) and MUAP duration and sEMG MPF (Figure 8 (b)). The inverse relationship between

MUAP duration and MPF has been previously demonstrated in simulation studies (Hermens et al. 1992; Lowery and O'Malley 2003), and investigated using dEMG techniques (Calder et al. 2008). However, the large sample population in this study enabled a significant correlation between the two parameters to be demonstrated experimentally for the first time. MUAP duration increased significantly immediately post-fatigue and returned to initial values after 10 minutes recovery (Figure 5 (b)). However, MUAP amplitude increased directly following the fatiguing contraction and remained elevated after the rest period (Figure 5 (c)), despite the median MU duration returning to pre-fatigue levels (Figure 5 (b)). This suggests that the increase in MUAP amplitude observed post-recovery is unlikely to be due to the ionic disturbances that alter MUAP waveforms during fatigue. A more plausible interpretation is that the increase in amplitude is predominantly due to the recruitment of additional large MUs to compensate for the reduction in the force generating capacity of the muscle, (Figure 6 (a)) (Bigland-Ritchie et al. 1986b; Carpentier et al. 2001; Enoka et al. 1989; Maton and Gamet 1989).

A uniform increase in the median and standard deviation of the MUAP durations was observed post-fatigue in Figure 4 (b). If larger MUs, associated with higher conduction velocities and shorter MUAP durations, are recruited to compensate for force loss, a greater range in the population durations may be expected. However, the results of this study support the findings of Gazzoni et al. (2005), who determined that changes in membrane properties due to the activity of recruited muscle fibers influence the conduction velocity of quiescent fibers and newly recruited motor units. Thus an increase in the duration of newly recruited MUAPs with respect to their durations in an unfatigued state would be expected, and is substantiated by the absence of lower range durations post-fatigue in this study, despite their presence before fatigue and after recovery.

Lastly, surface-detected action potentials from motor units located at greater depths within the muscle will tend to have larger durations due to the spatial low pass filtering effect of the tissue. The volume conductor effect means that MUAPs of deeper motor units will have longer durations and attenuated amplitudes with respect to more superficial units (Dimitrova and Dimitrov 2003; Lowery et al. 2002). The recruitment of motor units according to spatial distribution, however, is unlikely to bias the

overall result of the study, as the FDI muscle has been reported to have a uniform distribution of large and small motor units, with the muscle fibers that comprise each unit widely dispersed (Milner-Brown and Stein 1975).

While the changes in motor unit duration during fatigue are well-established, the variations in MUAP amplitude are less clear. Evidence for peripheral factors inducing changes in MUAP amplitude during fatigue can be found in the literature. A decline in M-wave amplitude has been reported directly after fatiguing contractions when there remained a strong influence of ion channel activity and concentration gradients on the intracellular action potential (Carpentier et al. 2001; Fuglevand et al. 1993a). A full recovery of the M-wave has been demonstrated after a 10 minute rest period (Fuglevand and Keen 2003; Post et al. 2008), indicating that the restoration of membrane excitability follows a similar time course. The recovery of MPF (Figure 2 (a)), and action potential duration (Figure 6 (b)), after the rest period in the present study suggest the ionic and metabolic changes are unlikely to have substantially influenced the increased sEMG and MUAP amplitudes following recovery.

Response to the Impairment of Muscle Force Generating Capacity

It is not possible to infer from the sEMG and MUAPs parameters whether one single mechanism or a combination of mechanisms is responsible for the decrease of the mechanical muscle force (Allen et al. 2008; Enoka and Duchateau 2008). Prolonged low-frequency force depression and reduced MVC and twitch force following sustained contractions have been previously attributed to excitation-contraction coupling failure in several studies (Hill et al. 2001; Westerblad et al. 1998). The prolonged reduction in the force generating capacity of the muscle is compensated by the recruitment of larger motor units, as reflected in the increase of the amplitude of the sEMG signal (Figure 2 (c)). A reduction in the threshold of MU activation for previously active MUs may be an additional compensatory strategy employed directly post-fatigue, where there is evidence of recruitment compression (Figure 7). The lowering of MU recruitment threshold may be peripherally mediated by changes in the mechanical and metabolic properties of the muscle, and could potentially counteract

the decline in force attributable to the reduction in MU firing rates. Despite the absence of recruitment compression post-recovery, the percentage increase in the mean amplitude of the MUs recruited at each threshold, averaged over all subjects, remained elevated, particularly at the latter stages of recruitment. This suggests that fatigue-induced lowering of the recruitment threshold of larger MUs was also employed post-recovery to compensate for the continued force impairment of those MUs already activated (Adam and De Luca 2003; Calder et al. 2008; Carpentier et al. 2001; Farina et al. 2009). The slope of the regression fit to the MUAP amplitude and threshold relationship exhibited an overall tendency to increase directly post-fatigue, which corresponds with the reported recruitment compression. However, across all subjects there was no systematic change observed in the slope of the regression fit after the recovery period, which implies that the compensatory strategies employed to cope with a force deficit may be specific to the individual. Supplementary MU activation and lower MU recruitment thresholds could both be present in varying combinations after fatigue.

Firing Rate and Uniformity of Changes

The current study offers a more comprehensive insight into firing rate alterations after muscle fatigue than previous reports on pooled single motor unit observations, by simultaneously examining the firing patterns of hundreds of motor units in each condition, across all subjects. In addition, the recording configuration allows the uniformity of motor unit adaptations to be investigated across a sample population with different thresholds of recruitment. The reduction in the mean MU firing rates observed following fatigue mirrors previous studies reporting an overall decline in MU discharge rates with the development of fatigue (Calder et al. 2008; Christova and Kossev 1998; Stock et al. 2012). Furthermore, average MU firing rates were consistently lower over the range of MU recruitment thresholds (Figure 6 (b)), which suggests that the reported decline was not a simply a consequence of the lower discharge rates of newly recruited MUs. Although previous studies have shown that newly recruited MUs can increase their discharge rate as fatigue progresses (Adam and De Luca 2005; Garland et al. 1994), the results of this study show that over the MU population discharge rates display a uniform reduction in response to fatigue (Figure 6 (b)). The reduction in discharge

517 frequency may occur as a result of a decline in the intrinsic excitability of MUs with previous activity
518 (Kernell and Monster 1982), or alternatively, firing rate may be modulated by inhibitory afferent
519 signals from receptors sensitive either to changes in the muscle contractile properties or to the
520 metabolic state of the muscle (Bigland-Ritchie et al. 1986a). In this study, alterations to MU
521 discharge rates were negatively correlated with changes in MUAP duration, which may imply a role
522 for metabolically activated inhibitory inputs in regulating MU firing. Proprioceptive feedback from
523 muscle spindles (De Luca and Kline 2012) and Golgi tendon organs (Kirsch and Rymer 1987) may
524 also contribute to the control of MU activity, although simultaneous recovery of firing rate and
525 MUAP duration was observed after rest with only partial restoration of force.

526 There were no consistent trends in the alterations to MU discharge rate or MUAP amplitude or
527 duration to suggest that higher threshold MUs were systematically more affected by fatigue, and
528 results varied by subject. This finding may be due to the low target force of the 20% MVC test
529 contractions sampling a relatively homogeneous group of fatigue-resistant MUs. Alternatively, the
530 longer hold phase of the fatigue task may have resulted in all detected MUs being active for similar
531 durations, thus the activity dependent adjustments would be comparable across the MU pool. Lastly,
532 it is likely that the intensity of the fatigue task induced widespread changes in the conduction velocity
533 of all muscle fibers and was not confined to distinct motor unit territories.

534 **CONCLUSION**

535 This study is the first to simultaneously examine global sEMG and the properties of a large population
536 of individual MUAPs, complete with recruitment threshold and firing rate information, before and
537 immediately after a sustained isometric fatiguing contraction, and following a recovery period.
538 Changes in the properties of the recruited motor unit population were found to be consistent with
539 alterations observed in the global EMG signal and displayed well-established manifestations of
540 fatigue over a large MU population. The observed increase in sEMG and MUAP amplitude post-
541 fatigue is consistent with previous studies that have demonstrated MU recruitment during fatiguing
542 contractions using intramuscular, conventional surface EMG and surface decomposition techniques.

MUAP duration and MPF were restored to initial pre-fatigue values following the rest period, suggesting that the fatigue-induced ionic and metabolic alterations that affect MFCV have also recovered. Despite the increase in central drive post-fatigue, motor unit firing rates were reduced, implying that to maintain force during fatigue, recruitment is favored over rate-coding while motor units are available. The presence of recruitment compression post fatigue may imply a peripherally mediated lowering of the MU recruitment threshold as an additional short-term compensatory mechanism to cope with large fatigue-induced force deficits. Though recruitment compression was absent after the recovery period, sEMG and MUAP amplitude remained elevated, and additional recruitment was still required to compensate for the continued impairment to the force. Motor unit discharge rates returned to initial values after rest, mirroring the recovery of MFCV. This provides evidence that the changes in MU firing are modulated by inhibitory afferents sensitive to the metabolic state of the muscle. In conclusion, this study employs sEMG decomposition techniques to examine fatigue-induced changes in the properties of a motor unit population and outlines possible recruitment strategies that may be employed to compensate for force deficits due to both short-term alterations in the metabolic state of the muscle and long-term variations in muscle contractile properties.

560 **REFERENCES**

561 **Adam A, and De Luca CJ**. Firing rates of motor units in human vastus lateralis muscle during
562 fatiguing isometric contractions. *Journal of Applied Physiology* 99: 268-280, 2005.
563 **Adam A, and De Luca CJ**. Recruitment order of motor units in human vastus lateralis muscle is
564 maintained during fatiguing contractions. *Journal of neurophysiology* 90: 2919-2927, 2003.
565 **Allen DG, Lamb G, and Westerblad H**. Skeletal muscle fatigue: cellular mechanisms. *Physiological*
566 *reviews* 88: 287-332, 2008.
567 **Beck TW, Kasishke PR, Stock MS, and DeFreitas JM**. Eccentric exercise does not affect common
568 drive in the biceps brachii. *Muscle & nerve* 46: 759-766, 2012.
569 **Bigland-Ritchie B, Dawson N, Johansson R, and Lippold O**. Reflex origin for the slowing of
570 motoneurone firing rates in fatigue of human voluntary contractions. *The Journal of physiology* 379:
571 451-459, 1986a.
572 **Bigland-Ritchie B, Furbush F, and Woods J**. Fatigue of intermittent submaximal voluntary
573 contractions central and peripheral factors. *Journal of Applied Physiology* 61: 421-429, 1986b.
574 **Calder KM, Stashuk DW, and McLean L**. Physiological characteristics of motor units in the
575 brachioradialis muscle across fatiguing low-level isometric contractions. *Journal of*
576 *Electromyography and Kinesiology* 18: 2-15, 2008.
577 **Carpentier A, Duchateau J, and Hainaut K**. Motor unit behaviour and contractile changes during
578 fatigue in the human first dorsal interosseus. *The Journal of physiology* 534: 903-912, 2001.
579 **Christova P, and Kossev A**. Motor unit activity during long-lasting intermittent muscle contractions
580 in humans. *European journal of applied physiology and occupational physiology* 77: 379-387, 1998.
581 **De Luca C, and Kline J**. Influence of proprioceptive feedback on the firing rate and recruitment of
582 motoneurons. *Journal of neural engineering* 9: 016007, 2012.
583 **De Luca CJ, and Hostage EC**. Relationship between firing rate and recruitment threshold of
584 motoneurons in voluntary isometric contractions. *Journal of neurophysiology* 104: 1034-1046, 2010.

De Luca CJ, and Nawab SH. Reply to Farina and Enoka: the reconstruct-and-test approach is the most appropriate validation for surface EMG signal decomposition to date. *Journal of neurophysiology* 105: 983-984, 2011.

Defreitas JM, Beck TW, Ye X, and Stock MS. Synchronization of low‐and high‐threshold motor units. *Muscle & nerve* 49: 575-583, 2014.

Dimitrova N, and Dimitrov G. Interpretation of EMG changes with fatigue: facts, pitfalls, and fallacies. *Journal of Electromyography and Kinesiology* 13: 13-36, 2003.

Dorfman LJ, Howard JE, and McGill KC. Triphasic behavioral response of motor units to submaximal fatiguing exercise. *Muscle & nerve* 13: 621-628, 1990.

Enoka RM, and Duchateau J. Muscle fatigue: what, why and how it influences muscle function. *The Journal of physiology* 586: 11-23, 2008.

Enoka RM, Robinson GA, and Kossev AR. Task and fatigue effects on low-threshold motor units in human hand muscle. *J Neurophysiol* 62: 1344-1359, 1989.

Esposito F, Orizio C, and Veicsteinas A. Electromyogram and mechanomyogram changes in fresh and fatigued muscle during sustained contraction in men. *European journal of applied physiology and occupational physiology* 78: 494-501, 1998.

Farina D, Holobar A, Gazzoni M, Zazula D, Merletti R, and Enoka RM. Adjustments differ among low-threshold motor units during intermittent, isometric contractions. *Journal of neurophysiology* 101: 350-359, 2009.

Farina D, Merletti R, and Enoka RM. The extraction of neural strategies from the surface EMG. *Journal of Applied Physiology* 96: 1486-1495, 2004.

Fuglevand A, Zackowski K, Huey K, and Enoka R. Impairment of neuromuscular propagation during human fatiguing contractions at submaximal forces. *The Journal of physiology* 460: 549-572, 1993a.

Fuglevand AJ, and Keen DA. Re-evaluation of muscle wisdom in the human adductor pollicis using physiological rates of stimulation. *The Journal of physiology* 549: 865-875, 2003.

Fuglevand AJ, Winter DA, and Patla AE. Models of recruitment and rate coding organization in motor-unit pools. *Journal of neurophysiology* 70: 2470-2488, 1993b.

Gabriel DA, and Kamen G. Experimental and modeling investigation of spectral compression of biceps brachii SEMG activity with increasing force levels. *Journal of Electromyography and Kinesiology* 19: 437-448, 2009.

Garland S, Enoka R, Serrano L, and Robinson G. Behavior of motor units in human biceps brachii during a submaximal fatiguing contraction. *Journal of Applied Physiology* 76: 2411-2419, 1994.

Gazzoni M, Camelia F, and Farina D. Conduction velocity of quiescent muscle fibers decreases during sustained contraction. *Journal of neurophysiology* 94: 387-394, 2005.

Gazzoni M, Farina D, and Merletti R. A new method for the extraction and classification of single motor unit action potentials from surface EMG signals. *Journal of neuroscience methods* 136: 165-177, 2004.

Hermens H, Bruggen T, Baten C, Rutten W, and Boom H. The median frequency of the surface EMG power spectrum in relation to motor unit firing and action potential properties. *Journal of Electromyography and Kinesiology* 2: 15-25, 1992.

Hicks A, and McComas A. Increased sodium pump activity following repetitive stimulation of rat soleus muscles. *The Journal of physiology* 414: 337-349, 1989.

Hill CA, Thompson MW, Ruell PA, Thom JM, and White MJ. Sarcoplasmic reticulum function and muscle contractile character following fatiguing exercise in humans. *The Journal of physiology* 531: 871-878, 2001.

Hogrel J-Y. Use of surface EMG for studying motor unit recruitment during isometric linear force ramp. *Journal of Electromyography and Kinesiology* 13: 417-423, 2003.

Holobar A, Farina D, Gazzoni M, Merletti R, and Zazula D. Estimating motor unit discharge patterns from high-density surface electromyogram. *Clinical neurophysiology* 120: 551-562, 2009.

Holtermann A, Grönlund C, Karlsson JS, and Roeleveld K. Motor unit synchronization during fatigue: described with a novel sEMG method based on large motor unit samples. *Journal of Electromyography and Kinesiology* 19: 232-241, 2009.

Hu X, Rymer WZ, and Suresh NL. Accuracy assessment of a surface electromyogram decomposition system in human first dorsal interosseus muscle. *Journal of neural engineering* 11: 026007, 2014.

Hu X, Rymer WZ, and Suresh NL. Assessment of validity of a high-yield surface electromyogram decomposition. *Journal of neuroengineering and rehabilitation* 10: 99, 2013a.

Hu X, Rymer WZ, and Suresh NL. Reliability of spike triggered averaging of the surface electromyogram for motor unit action potential estimation. *Muscle & nerve* 48: 557-570, 2013b.

Hu X, Suresh AK, Li X, Rymer WZ, and Suresh NL. Impaired motor unit control in paretic muscle post stroke assessed using surface electromyography: a preliminary report. In: *Engineering in Medicine and Biology Society (EMBC), 2012 Annual International Conference of the IEEE*IEEE, 2012, p. 4116-4119.

Jensen B, Pilegaard M, and Sjøgaard G. Motor unit recruitment and rate coding in response to fatiguing shoulder abductions and subsequent recovery. *European journal of applied physiology* 83: 190-199, 2000.

Kallenberg LA, and Hermens HJ. Behaviour of a surface EMG based measure for motor control: Motor unit action potential rate in relation to force and muscle fatigue. *Journal of Electromyography and Kinesiology* 18: 780-788, 2008.

Kernell D, and Monster A. Time course and properties of late adaptation in spinal motoneurones of the cat. *Experimental brain research* 46: 191-196, 1982.

Kirsch R, and Rymer W. Neural compensation for muscular fatigue: evidence for significant force regulation in man. *J Neurophysiol* 57: 1893-1910, 1987.

Kleine BU, van Dijk JP, Zwarts MJ, and Stegeman DF. Inter-operator agreement in decomposition of motor unit firings from high-density surface EMG. *Journal of Electromyography and Kinesiology* 18: 652-661, 2008.

Lowery MM, Nolan P, and O'Malley MJ. Electromyogram median frequency, spectral compression and muscle fibre conduction velocity during sustained sub-maximal contraction of the brachioradialis muscle. *Journal of Electromyography and Kinesiology* 12: 111-118, 2002.

Lowery MM, and O'Malley MJ. Analysis and simulation of changes in EMG amplitude during high-level fatiguing contractions. *Biomedical Engineering, IEEE Transactions on* 50: 1052-1062, 2003.

Maton B, and Gamet D. The fatigability of two agonistic muscles in human isometric voluntary submaximal contraction: an EMG study. *European journal of applied physiology and occupational physiology* 58: 369-374, 1989.

Milner-Brown H, and Stein R. The relation between the surface electromyogram and muscular force. *The Journal of physiology* 246: 549-569, 1975.

Nawab SH, Chang S-S, and De Luca CJ. High-yield decomposition of surface EMG signals. *Clinical neurophysiology* 121: 1602-1615, 2010.

Post M, Bayrak S, Kernell D, and Zijdewind I. Contralateral muscle activity and fatigue in the human first dorsal interosseous muscle. *Journal of Applied Physiology* 105: 70-82, 2008.

Stock MS, Beck TW, and Defreitas JM. Effects of fatigue on motor unit firing rate versus recruitment threshold relationships. *Muscle & nerve* 45: 100-109, 2012.

Suresh N, Kuo A, Heckman C, Ellis M, and Rymer W. Correlation of mechanical action with directional tuning in the first dorsal interosseous (FDI). In: *Proceedings of the XIVth Congress of the International Society for Electrophysiology and Kinesiology*2002, p. 22-25.2002.

Thomas CK, Johansson RS, and Bigland-Ritchie B. EMG changes in human thenar motor units with force potentiation and fatigue. *Journal of neurophysiology* 95: 1518-1526, 2006.

Westerblad H, Allen D, Bruton J, Andrade F, and Lännergren J. Mechanisms underlying the reduction of isometric force in skeletal muscle fatigue. *Acta Physiologica Scandinavica* 162: 253-260, 1998.

FIGURE CAPTIONS

Figure 1. (a) Four channels of surface EMG recorded from the FDI using the Precision Decomposition System during a 20 second 20% MVC trapezoidal force trajectory (b).

Figure 2. Median values for (a) median power frequency and (b) root mean squared amplitude of the global surface EMG signal across all subjects for pre-fatigue, post-fatigue and recovery conditions. Median values were calculated from data recorded during the steady state hold (7-9 seconds) of the trapezoidal force trajectory. All values were standardized to the mean and standard deviation of pre-fatigue values. Significant differences at the $p < .05$ and $p < .005$ level are indicated with a single asterisk and a double asterisk respectively.

Figure 3. Probability distribution of MU amplitudes (a) for a single subject and (b) across all subjects. Boxplots display the mean (line), median ('+'), standard deviation and outliers of the distribution. MU amplitudes for each subject have been standardized to his or her pre-fatigue values for comparison. The asterisk indicates that for the post-fatigue and recovery conditions 6 and 7 MUAP amplitudes, respectively, were larger than 9.26.

Figure 4. Probability distribution of MU durations (a) for a single subject and (b) across all subjects. Boxplots display the mean (line), median ('+'), standard deviation and outliers of the distribution.

Figure 5. (a) Maximum voluntary contraction, (b) median MUAP duration and (c) median standardized MUAP amplitude for the decomposed motor unit action potentials across all subjects for pre-fatigue, post-fatigue and recovery conditions. Significant differences at the $p < .05$ and $p < .001$ level are indicated with a single asterisk and a double asterisk respectively.

Figure 6. (a) Distribution of mean MU firing rates across all subjects for pre-fatigue, post-fatigue and recovery conditions and (b) average firing rate of MUs binned with respect to the MU threshold of recruitment for all subjects. Significant differences at the $p < .05$ and $p < .001$ level are indicated with a single asterisk and a double asterisk respectively.

Figure 7. Probability distribution of MU recruitment thresholds (a) for a single subject and (b) across all subjects. Boxplots display the mean (line), median ('+'), standard deviation and outliers of the distribution.

Figure 8. Scatterplot of (a) the median decomposed MUAP amplitude and the RMS amplitude of the global sEMG signal for all subjects for each of the three conditions $r = .86$ and (b) the median decomposed MUAP duration and the MPF of the global sEMG signal for all subjects for each of the three conditions $r = -.95$.

716 **FIGURES**

717 Figure 1

718

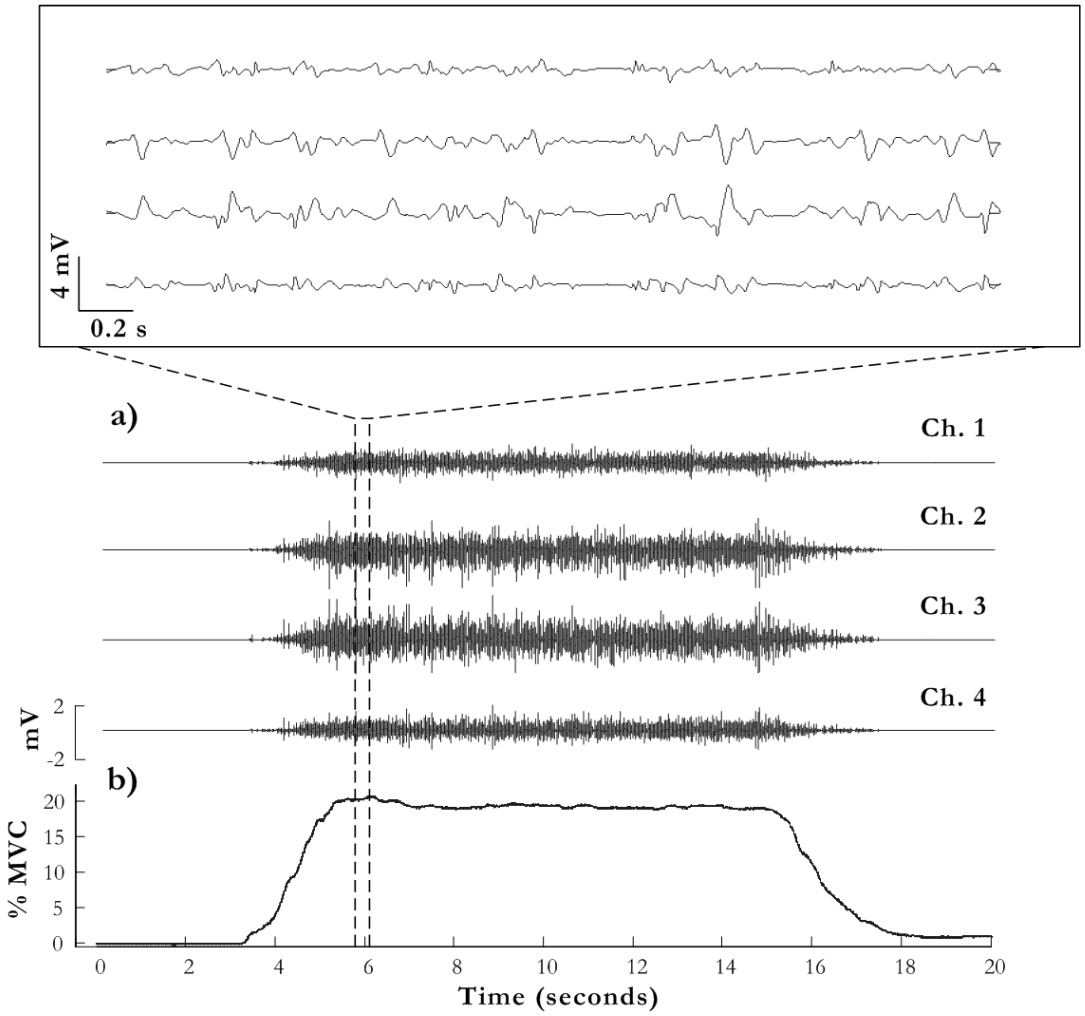

719

720

721 Figure 2

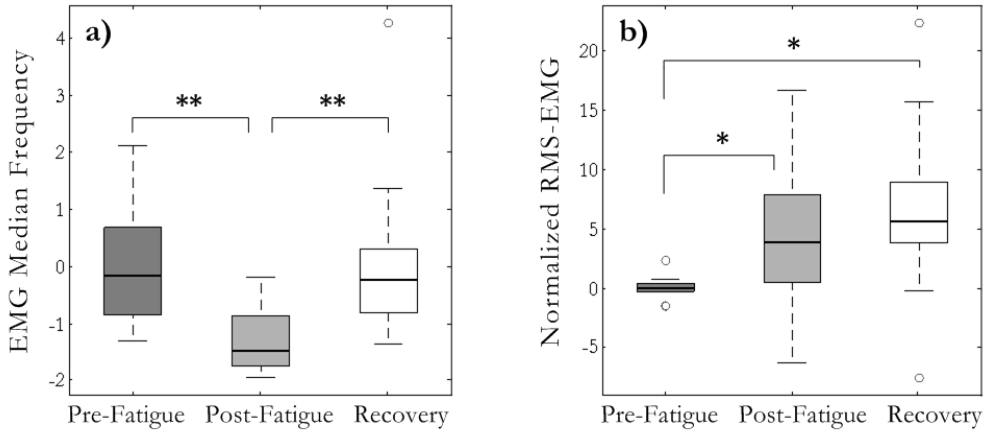

722

723

724 Figure 3

725

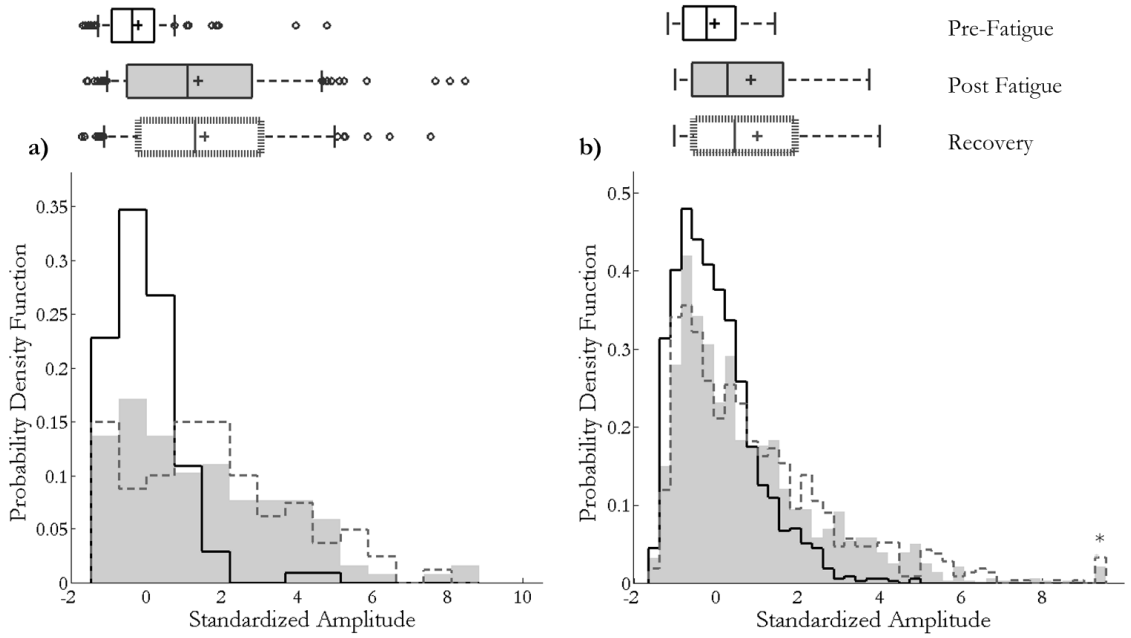

726

727

728

729 Figure 4

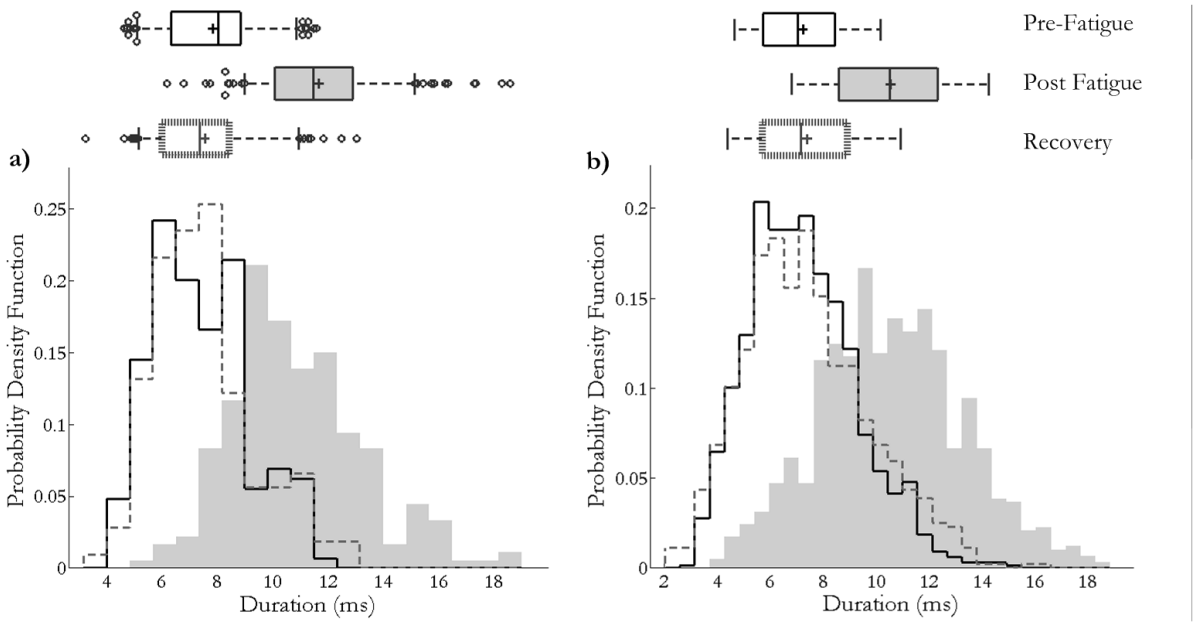

730

731

732 Figure 5

733

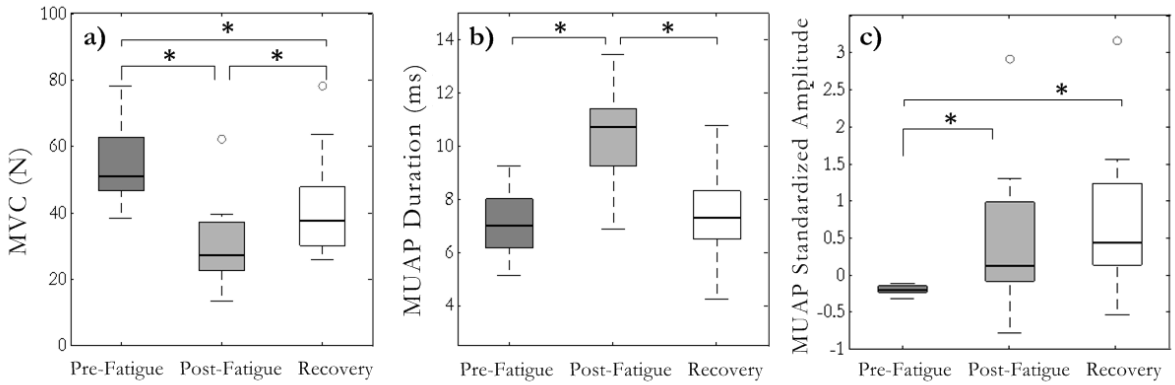

734

735

736 Figure 6

737

738

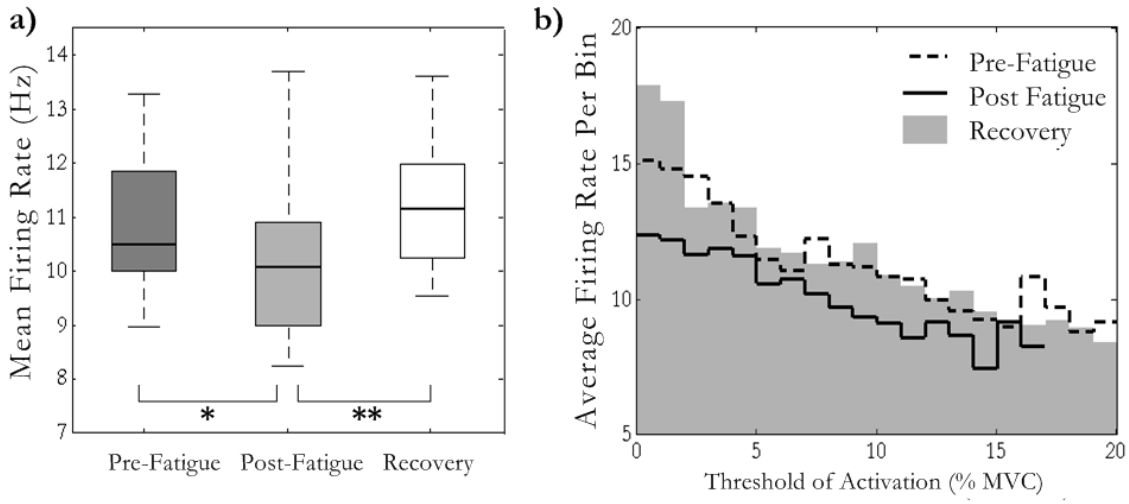

739

740

741 Figure 7

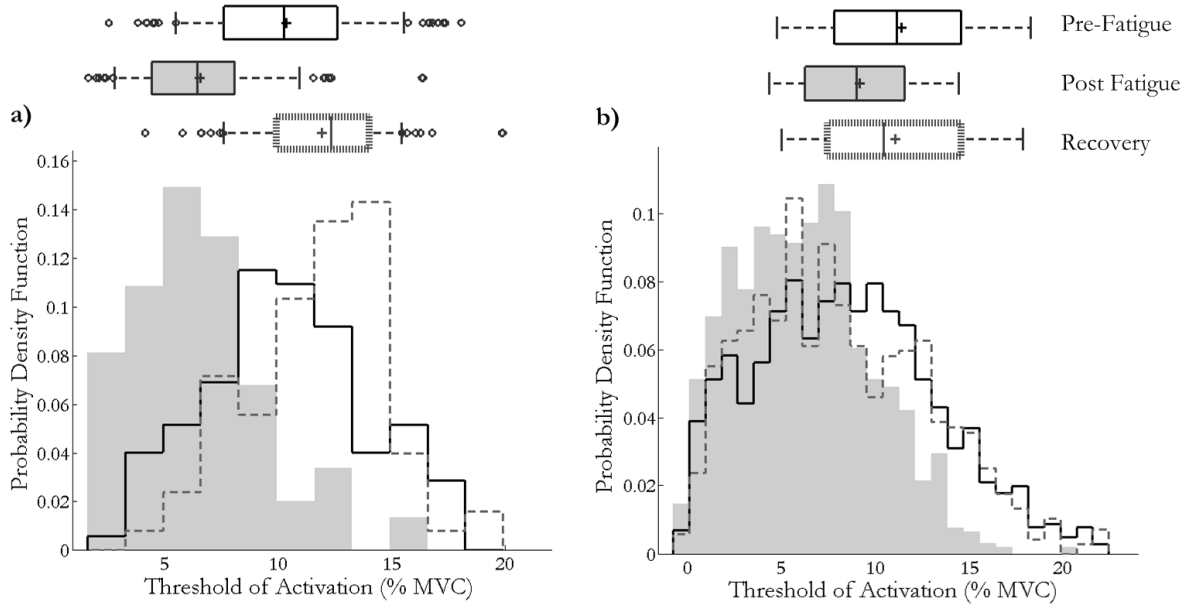

742

743

744 Figure 8

745

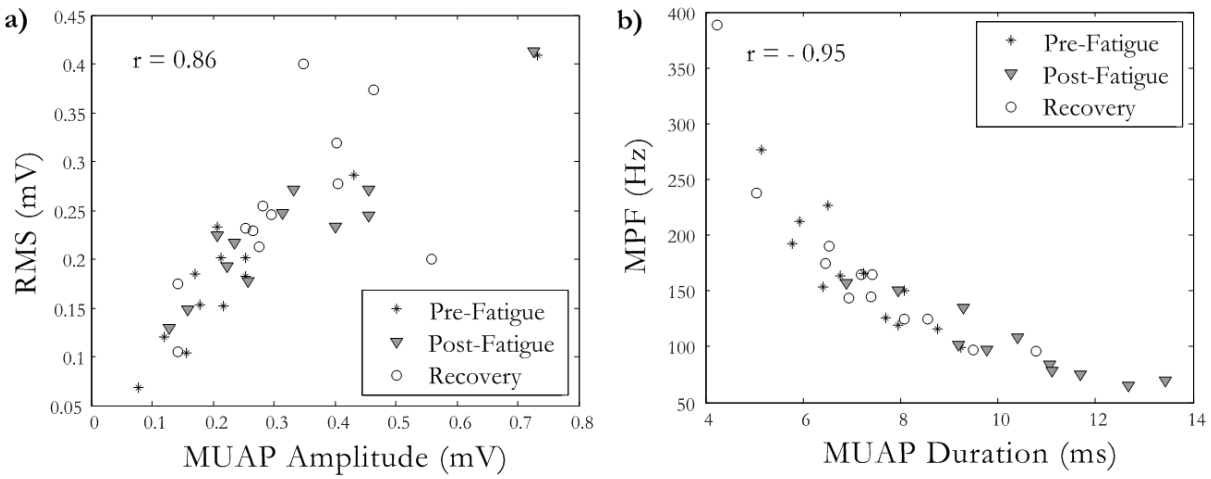

746